Original Article

Immature tertiary lymphoid structure formation was increased in the melanoma tumor microenvironment of *IKZF1* transgenic mice

Shanshan Yin[1], Chao Zhang[2], Fenghou Gao[1]

[1]Department of Oncology, Shanghai 9th People's Hospital, Shanghai Jiao Tong University School of Medicine, Shanghai, China; [2]Department of Geriatrics, Shanghai 9th People's Hospital, Shanghai Jiao Tong University School of Medicine, Shanghai, China

Contributions: (I) Conception and design: F Gao; (II) Administrative support: F Gao; (III) Provision of study materials or patients: C Zhang, F Gao; (IV) Collection and assembly of data: All authors; (V) Data analysis and interpretation: S Yin; (VI) Manuscript writing: All authors; (VII) Final approval of manuscript: All authors.

Correspondence to: Fenghou Gao. Department of Oncology, Shanghai 9th People's Hospital, Shanghai Jiao Tong University School of Medicine, Shanghai 201999, China. Email: fenghougao@163.com; Chao Zhang. Department of Geriatrics, Shanghai 9th People's Hospital, Shanghai Jiao Tong University School of Medicine, Shanghai 201999, China. Email: 2953982857@qq.com.

Background: *IKZF1* promotes the occurrence of lymphoma and is also related to the development of breast cancer, liver cancer, and ovarian cancer. It was hypothesized that *IKZF1* influences tertiary lymphoid structures (TLSs) formation and development in the tumor immune microenvironment, and this effect of *IKZF1* on the tumor immune microenvironment has not been explored. Using melanoma grafts as a model, we investigated the effect of *IKZF1* on the immune microenvironment of melanoma.

Methods: The Cell Count Kit-8 (CCK8) assay was used to detect the effect *IKZF1* overexpression in melanoma cells on cell proliferation. The *IKZF1* overexpression vector was constructed by homologous recombination. After linearization, the overexpression vector was microinjected into the fertilized egg. Transgenic mice overexpressing *IKZF1* were screened by tail identification. After melanoma B16 mouse cells were digested into single cells, the tumor was subcutaneously implanted in C57BL6/J-wild type (WT) mice and *IKZF1* transgenic mice, and the tumor growth of the 2 groups was compared. The number of TLSs in the tumor tissues of mice was analyzed after hematoxylin-eosin (HE) staining.

Results: Overexpression of *IKZF1* in melanoma cells did not affect cell proliferation. The *IKZF1* overexpression vector pcDNA3.1-CAG-IKAROS was successfully constructed. Viable fertilized eggs were obtained after microinjection. Transgenic mice stably expressing *IKZF1* were identified by polymerase chain reaction (PCR). Compared with WT mice, the tumor load of *IKZF1* transgenic mice increased significantly. HE staining showed that the number of immature TLSs in melanomas of *IKZF1* transgenic mice increased significantly.

Conclusions: *IKZF1* does not affect the proliferation of melanoma cells. Transgenic mice overexpressing *IKZF1* were successfully constructed. *IKZF1* is a key driver gene of the formation of immature TLS.

Keywords: *IKZF1*; tumor immune microenvironment; tertiary lymphoid structure (TLS); melanoma

Submitted Jun 01, 2022. Accepted for publication Jul 07, 2022.
doi: 10.21037/tcr-22-1759
View this article at: https://dx.doi.org/10.21037/tcr-22-1759

Introduction

With the clinical application of immunotherapy, the use of anti-cytotoxic T lymphocyte-associated protein 4 (*CTLA4*) or anti-programmed death receptor 1 (*PD-1*) antibodies provides effective treatment for some melanoma patients (1-4). The main reason for the efficacy of immune checkpoint therapy is the activation of the anti-tumor immune response (5,6). Tertiary lymphoid structures (TLSs) are the main reason for the efficacy of immune checkpoint

inhibitors (7-9).

TLSs are ectopic lymphoid organs that develop in chronic inflammatory sites such as tumors (10,11). TLSs can be divided into early TLSs (lymphocyte aggregates), primary TLSs (primary lymphoid follicles), and secondary TLSs (secondary lymphoid follicles) (10,12,13). Patients with TLSs with primary or secondary lymphoid follicle-like differentiation have a lower risk of recurrence than patients with liver cancer and colorectal cancer containing lymphocyte aggregates (10,13). TLS maturity is indicated by a germinal center (GC). The mature state of TLSs may affect their prognostic value (10). An increase in mature TLS indicates a favorable prognosis and is the result of a positive response to immune checkpoint inhibitors. As a result, clinical detection of the types and number of TLS in tumor samples can indirectly support immunotherapy response, and investigating the factors and methods that drive the formation of TLS in tumor microenvironment can become a direction of current tumor immunotherapy development.

IKZF1 is a transcription factor of the zinc finger protein family (14). IKZF1 promotes the occurrence of lymphoma and is also related to the development of breast cancer, liver cancer, and ovarian cancer (15). IKZF1 is an essential regulator of lymphocyte differentiation, loss of IKZF1 activity results in profound differentiation defects and leukemic transformation of B and T cell precursors (16). IKZF1 also promotes B-cell proliferation and differentiation by activating kinase signaling cascades and cooperating with chromatin protein 4 (17). IKZF1 participates in the regulation of differentiation of neutrophils by silencing permissible or specific pathways in the ordinary precursors of macrophage-monocyte evolution (18). It's speculated that IKZF1 regulates the differentiation of multiple immune cells in the tumor immune microenvironment. TLSs are lymphocyte and tissue regeneration induced by inflammatory states such as tumors (10,11). IKZF1 regulates normal lymphocyte development and differentiation, and overexpression of IKZF1 promotes lymphoma growth (15,16). Based on the facts it is thought that IKZF1 may affect the tumor immune microenvironment as well as the formation and development of TLS. The association of IKZF1 and TLS needs to be interpreted in the melanoma microenvironment.

Therefore, this study intends to observe the effect of IKZF1 overexpression on the proliferation of melanoma cells. Generating transgenic mice with overexpression of IKZF1 and exploring the impact of IKZF1 on the melanoma tumor immune microenvironment. Our findings and data can provide new ideas for regulating the melanoma tumor immune microenvironment by targeting IKZF1. We present the following article in accordance with the ARRIVE reporting checklist (available at https://tcr.amegroups.com/article/view/10.21037/tcr-22-1759/rc).

Methods

Materials

Experimental animals

Specific pathogen free (SPF) C57BL/6 mice aged 6–9 weeks were purchased from Shanghai Southern Model Biology Research Center. All mice were reared in the SPF level barrier environment in the northern animal room of the Ninth People's Hospital Affiliated to Shanghai Jiao Tong University School of Medicine. The barrier temperature was 20–24 ℃, the humidity was 45–65%, and the day and night cycle was alternated (12 h:12 h). The mice were free to eat food and water, and 3–6 mice were reared in each cage. Animal experiments were performed under a project license (No. SH9H-2020-A276-1) granted by the Experimental Animals Ethics Committee of Shanghai 9th People's Hospital, Shanghai Jiao Tong University School of Medicine, in compliance with the national guidelines for the care and use of animals.

Reagents and instruments

Plasmid pcDNA3.1 was purchased from Invitrogen. Plasmid pcDNA3.1-CAG was reconstructed by Dr. Sunrui Lin of the Shanghai Model Organisms Center. DH5α competent cells were purchased from TransGen Biotech. Various restriction endonucleases, recombinant enzymes, Taq enzymes, gel recovery kits, and other PCR-related reagents were purchased from TaKaRa company. The Plasmid Extraction kit was purchased from Qiagen company. The CCK8 kit was purchased from Dojindo company. Actin and Flag antibodies used in Western blot were purchased from Cell Signaling Technology. The chemical reagents configured with M16 and M2 culture solutions were purchased from Sigma. Hematoxylin staining solution, differentiation solution, and blue returning solution were purchased from Shanghai Ruiyu Biotechnology Co., Ltd., and xylene, absolute ethanol, 3% H_2O_2, and other hematoxylin-eosin (HE) staining-related reagents were purchased from Sinopharm Chemical Reagent Co., Ltd. The main instruments included the PCR

instrument (ABI company of the United States), DNA electrophoresis tank (Shanghai Tianneng Technology Co., Ltd.), gel imaging system (Cytiva company of the United States), tissue spreader (Huasu Technology Co., Ltd. of Jinhua City, Zhejiang Province), panoramic scanner (Ningbo Jiangfeng Biology Co., Ltd.), frozen platform (Wuhan Junjie Electronics Co., Ltd.), embedding machine (Tianjin Tianli Aviation Electromechanical Co., Ltd.), pathological slicer (Shenyang Yude Electronic Instrument Co., Ltd.), optical microscope (Nikon company, New York, America), and imaging system (Nikon company).

Research method

Construction of the transgenic plasmid

Amplification was carried out according to the coding sequence (CDS) sequence of the mouse *IKAROS* gene (NM 001301865.1). The upstream primer (*IKAROS*-F) was 5'-ATCACGAGACTAGCCTCGAGATGGACTAC AAGGACGATGATGACAAGGATGTCGATGAGGG TCAAGAC-3'. The downstream primer (*IKAROS*-R) was 5'-CTTAAGCTTGGTACCTTAGCTCAGGTGGTA ACGATG-3'. The primer was synthesized by Shanghai Sangong Bioengineering Co., Ltd., and the expected length of the amplified target fragment was 1,346 bp. C57BL/6J mouse mRNA was extracted and reverse-transcribed with a reverse transcription kit. The reverse-transcribed cDNA was used as a template and amplified with the homologous arm amplification primers described above and recovered. The pcDNA3.1-CAG vector was digested with Xho I and Kpn I at 37 ℃ for 3 h. The digested products were identified by 1% agarose gel electrophoresis, and then the gel was recovered. The amplified *IKAROS* fragment and the digested pcDNA3.1-CAG vector were homologously recombined under the action of the recombinant enzyme. The recombinant plasmid was transformed into DH5α *E. Coli* bacteria for extended culture, and then plasmids were extracted and sent to Sangong Biotech Co., Ltd. (Shanghai) for sequencing. The strains with the correct plasmids were cultured again to extract the endotoxin-free pcDNA3.1-CAG-*IKAROS* plasmid.

Construction of the *IKZF1* gene overexpression plasmid

The vector pSIN was digested by EcoRI and BamHI, and homologous recombination was carried out with the amplified *IKZF1* fragment under the action of the recombinant enzyme. The upstream primer (*IKZF1*-3FLAG-F) was 5'-GGGCTAGCTAGCTAGGAATTCA TGGACTACAAAGACGATGACGACAAGGACTACA AAGACGATGACGACAAGGACTACAAAGACGATGA CGACAAGATGGATGTCGATGAGGGTC-3', and the downstream primer (*IKZF1*-R) was 5'-GCCCTAGATGCA TGCGGATCCTTAGCTCAGGTGGTAACG-3'.

CCK8 proliferation assay

Negative control (NC) cells in the logarithmic phase of growth and melanoma cells overexpressing *IKZF1* were digested into single cells and diluted to a cell density of 3,000 cells/100 μL. The cell suspension was added to 96-well plates. Sterile phosphate-buffered saline (PBS) buffer (100 μL) was added into the outermost wells of the 96-well plates to prevent excessive evaporation of the culture medium, which affects the accuracy of the test. CCK8 test reagent (10 μL) was added to each well. The plate was gently pat to fully mix the reagent with the culture medium and avoid bubbles. The 96-well plates were put back into the constant temperature incubator and continued to incubate for 2 h before testing.

Western blotting

Cell precipitates were collected and 2× sodium lauryl sulfate (SDS) lysis buffer was added to split and collect the supernatant. Separation and concentrated gels with appropriate concentration were prepared, and the target proteins were separated by polyacrylamide gel electrophoresis. The gel was transferred to the polyvinylidene fluoride (PVDF) membrane, and 5% milk was used for blocking at room temperature for 1 h. The primary antibody and corresponding secondary antibody were added to the membrane and incubated. Immobilon Western chemiluminescent horseradish peroxidase (HRP) substrate was used to identify immunoreactive bands (Millipore Co., USA).

Preparation of transgenic mice

The transgenic plasmid was digested with SspI, and a 7.862 kb DNA fragment was recovered for microinjection. After superovulation, C57BL/6J female mice aged 5–6 weeks were mated with mature C57BL/6J male mice. The embolus mice were selected, and the fertilized eggs with normal morphology were collected, screened, and cultured in M16 medium. The linearized and purified plasmid DNA was diluted with Tris-EDTA (TE) buffer to a concentration of 5 ng/μL. DNA was injected into the male pronucleus of the fertilized egg with M2 as the *in vitro* operating fluid.

At the same time, pseudopregnant mice were obtained by selecting suitable age female mice that could mate with vas deferens-ligated male mice. The injected fertilized eggs were transplanted into the fallopian tubes of 0.5-day-old pseudopregnant mice. About 25 eggs were transferred unilaterally from the fallopian tubes of each pseudopregnant mouse. Whether the recipient mother was pregnant and its individual development were observed.

Identification of *IKZF1* gene transgenic mice

When the mice grew to about 4 weeks, their tails were cut for genotype identification. After wiping the tail with alcohol, a 1–5 mm section of the tail of newborn mice was cut with scissors and placed into a 2-mL EP tube, then numbered accordingly. Subsequently, 85 μL lysis buffer was added to the 2-mL EP tube and gently vortexed to completely soak the sample in lysate, followed by brief centrifugation. The tissue was infiltrated below the lysate level. After incubation at 95 ℃ for 15 min in the constant temperature incubator, 10 μL termination buffer was added to terminate the lysis. The tube was centrifuged at a speed of 11,000 g for 5 min and the supernatant was aspirated into a new EP tube. Genomic DNA for later identification was temporarily stored at 4 ℃. The PCR amplification conditions for gene identification were as follows: 94 ℃ 30 s, 63.6 ℃ 30 s, 72 ℃ 1 min, a total of 35 cycles. The primer sequence was as follows: CAG-1 5'-ATCACGAGACTAGCCTCGAGG-3', *IKZF1* 5'-ATGCGGGTTGATGTGGTTGGTTAG-3'. Transgenic positive mice should have an amplified 1,060 bp product. PCR products were identified with 1% agarose gel.

Animal model preparation

Three male *IKZF1* transgenic mice aged 6–8 weeks and 3 C57BL6/J wild-type (WT) mice were selected and placed in separate cages 1 week before the experiment. The tumor volume was measured in each mouse with 1×10^6 B16 cells after tumor formation was initiated subcutaneously.

HE staining and TLS counting

The tumor wax blocks were cut into sections and then baked. They were dewaxed with xylene, absolute ethanol, 90% ethanol, 70% ethanol, and pure water. Hematoxylin was dyed for 10 min and eosin was dyed for 30 s. 95% ethanol, 100% ethanol and xylene were used for dehydration and transparency. After sealing with neutral resin, samples were observed under a microscope.

Two pathologists with extensive pathology experience examined the slides with HE staining independently. A previously published scale was used to assess the presence of intra-tumoral TLSs on hematein-eosin-saffron stained slides. TLSs were classified as follows: (I) aggregates: vague, ill-defined lymphocyte clusters; (II) primary follicles: round-shaped lymphocyte clusters without GC formation; and (III) secondary follicles: follicles with GC formation (13).

Statistical analysis

The statistical analysis software GraphPad Prism was used for analysis and statistics. The results were expressed in the form of mean ± standard deviation. The *t*-test was used to compare differences between the 2 groups. When $P<0.05$, the difference was statistically significant (*, $P<0.05$; **, $P<0.01$; ***, $P<0.001$).

Results

Overexpression of IKZF1 gene in melanoma cells did not affect cell proliferation

After the melanoma cell line B16 was transfected with *IKZF1* overexpression plasmid, the expression of Flag-*IKZF1* protein was detected by Western blot, and the B16 cell line with *IKZF1* overexpression was successfully constructed (*Figure 1A*). The CCK8 assay showed that compared with the control group, *IKZF1* overexpression resulted in no significant change in cell proliferation (*Figure 1B*).

Construction of the pcDNA3.1-CAG-IKAROS plasmid

The pcDNA3.1-CAG-*IKAROS* recombinant plasmid was generated by homologous recombination of purified and recovered *IKZF1* sequence fragment and pcDNA3.1-CAG vector fragment (*Figure 2A*). Through agarose gel identification, a 7.862 kb positive band appeared in lane 2, indicating that the corresponding product contained the targeted recombinant plasmid (*Figure 2B*). The positive clones were sequenced, and the recombinant plasmid was successfully constructed.

Identification of IKZF1 gene overexpression transgenic positive mice and mice genotypes after amplification and breeding

The linearized recombinant plasmid (*Figure 2B*) was injected into the male pronucleus of the fertilized egg of the donor mouse by microinjection. A total of 300 surviving

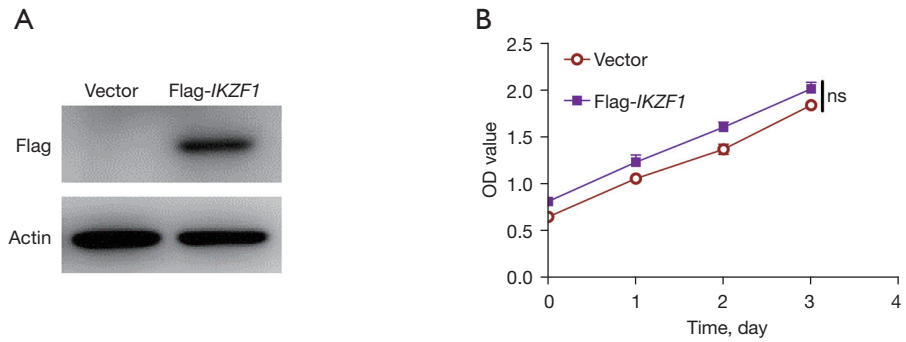

Figure 1 *IKZF1* overexpression in melanoma cells did not affect cell proliferation. (A) After B16 cells were transfected with *IKZF1* overexpression plasmid, the expression of the Flag-*IKZF1* protein was detected by Western blot. (B) The CCK-8 assay detected the proliferation of B16-Vector and B16-Flag-*IKZF1* cells. ns, not significant; CCK-8, Cell Count Kit-8; OD, optical density.

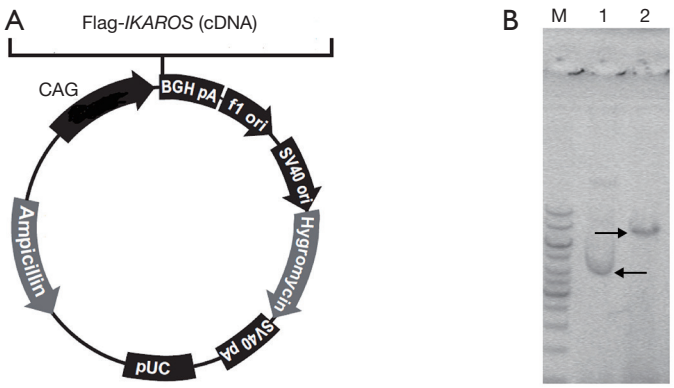

Figure 2 PCR identification of the pcDNA3.1-CAG-*IKAROS* sequence. (A) Schematic diagram of pcDNA3.1-CAG-*IKAROS* recombinant plasmid. (B) Agarose gel electrophoresis results of the recombinant plasmid, where lane 1 is the DNA marker MBI GeneRuler 1,000 bp. The lane 2 is the pcDNA3.1-CAG-*IKAROS* PCR product, the arrow below indicates the position. The lane 3 is pcDNA3.1-CAG-*IKAROS* after SspI single enzyme digestion, the arrow above indicate location. M, marker; PCR, polymerase chain reaction.

fertilized eggs were obtained and transplanted into 25 pseudopregnant female mice, of which 19 were pregnant, with a pregnancy rate of 76%. The genomic DNA of the mouse tail was extracted for PCR identification. The results are shown in *Figure 3A*, and a 1,060 bp band was amplified. This indicated a transgenic positive mouse with overexpression of *IKZF1*. The *Figure 3A* showed that lanes 1–5 were the positive first establishment mice (F0) with overexpression of *IKZF1*, lane 6 was the NC, lane 7 was the blank control, lane 8 was the positive control, and lane 9 was the DNA marker. The information of the first mice is shown in *Figure 3B*. F1 generation mice were bred by mating the first established mice with WT C57BL/6J mice. The same method was used for PCR identification as for screening F0 positive mice, and subsequent experiments could be carried out after stable passage.

The weight of transplanted tumors increased significantly after IKZF1 gene transgenic mice were inoculated with melanoma cells

The tumor tissue was removed after B16 tumour was implanted in WT mice and *IKZF1* transgenic mice, and *IKZF1* transgenic mice had a higher tumor load than the WT mice (*Figure 4*).

Increased immature TLS formation in the transplanted tumors of IKZF1 gene transgenic mice

To understand the mechanism of faster growth of melanoma in *IKZF1* overexpression transgenic mice, we obtained tumor tissues of WT and *IKZF1* transgenic mice for HE staining. The results showed that, compared with WT

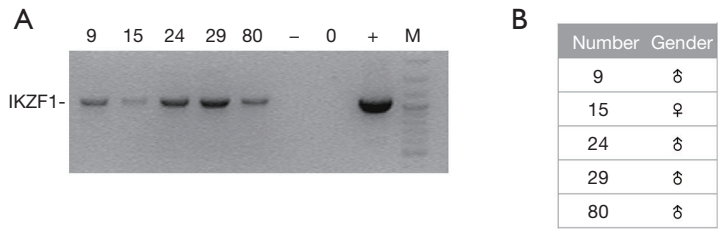

Number	Gender
9	♂
15	♀
24	♂
29	♂
80	♂

Figure 3 The genotype identification of *IKZF1* transgenic mice. (A) Genotype identification results of *IKZF1* transgenic mice. (B) Information of the first mouse. M, marker; –, negative control; +, positive control; ♀, female mice; ♂, male mice.

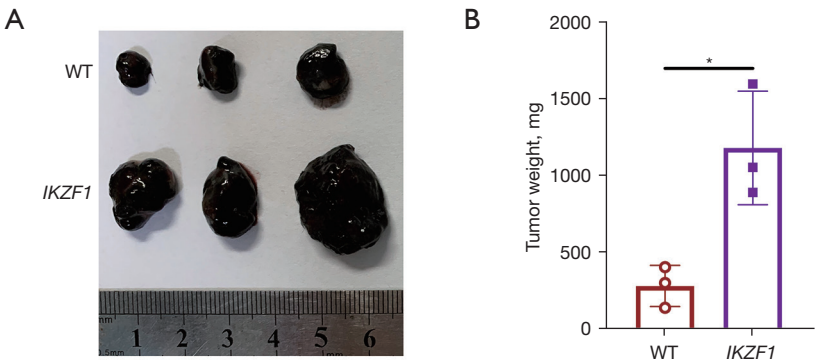

Figure 4 The weight of transplanted tumors increased significantly after the *IKZF1* transgenic mice were inoculated with melanoma cells. Tumor weight of WT and *IKZF1* transgenic mice bearing B16 cells. *, P<0.05. WT, wild type.

mice, the number of lymphocytes aggregated, and primary lymphoid follicles and secondary lymphoid follicles in melanomas of *IKZF1* transgenic mice changed. The number of lymphocyte aggregates in transplanted tumors of *IKZF1* transgenic mice increased significantly, while the number of primary lymphoid follicles did not change significantly (*Figure 5*). No statistical analysis was performed due to the small number of secondary lymphoid follicles in the transplanted tumors of transgenic mice and WT mice.

Discussion

Our study showed that after overexpression of *IKZF1* in mouse melanoma cells, *IKZF1* had no significant effect on tumor proliferation. In previous studies, *IKZF1* is a gene closely related to tumor development. High expression of *IKZF1* in ovarian serous adenocarcinoma leads to enhanced cell invasion and metastasis (19). The increased expression of *IKZF1* is related to the recurrence and metastasis of lung adenocarcinoma and is involved in its progression (20). *IKZF1* is highly expressed in multiple myeloma. Targeted inhibition of *IKZF1* by lenalidomide can effectively prolong the survival time of multiple myeloma (21). This inconsistency could be attributed to the different effects of *IKZF1* in different tumor types. *IKZF1* is speculated to affect tumors by influencing the tumor microenvironment in our research model.

To explore whether *IKZF1* affects the occurrence of tumors through the tumor microenvironment, we successfully constructed *IKZF1* transgenic mice. The successful *IKZF1* transgenic mouse model was inoculated with melanoma cells to observe melanoma growth. Compared with WT mice, the melanomas of *IKZF1* overexpression transgenic mice had a greater tumor load. Therefore, *IKZF1* may affect tumor growth through the tumor microenvironment. The tumor microenvironment refers to the cellular environment in which tumors exist, mainly including tumor cells, immune cells, stromal cells, extracellular matrix and secretory molecules, and blood and lymphatic vessels. Numerous types of cells and extracellular matrices regulate and interact with each other at various levels and scales and jointly shape the tumor microenvironment (22-26). When the tumor microenvironment is related to the function and signal

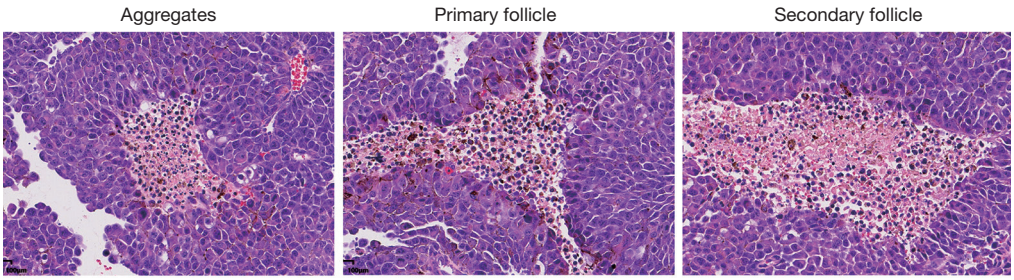

	WT			*IKZF1*		
Number	1	2	3	1	2	3
Aggregates	27	6	24	79	76	61
Primary follicle	6	1	4	2	1	0
Secondary follicle	1	0	0	0	0	0

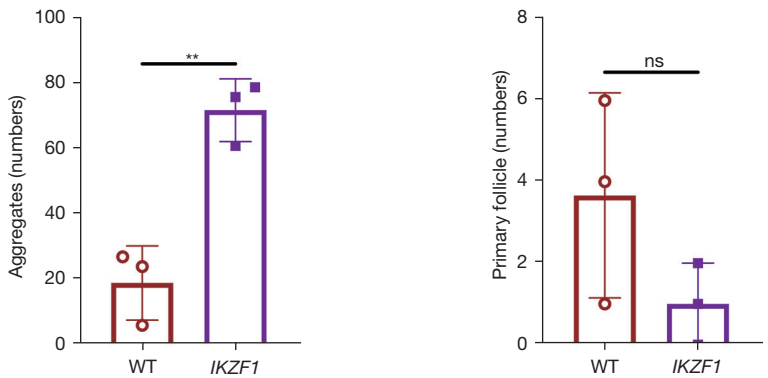

Figure 5 Immature tertiary lymphoid structure formation was increased in the melanomas of *IKZF1* transgenic mice. After HE staining, TLSs was observed under microscope (×20). **, P<0.01. ns, not significant; WT, wild type; HE, hematoxylin-eosin; TLSs, tertiary lymphoid structures.

exchange of immune cells, it can also be called the tumor immune microenvironment. The tumor immune microenvironment contains cellular components that play an immunosuppressive role, as well as anti-tumor immune components, such as TLSs. Mature TLSs (secondary TLSs) are comprised of follicular dendritic cells (FDCs) and GCs. These FDCs are adjacent to a small T cell region, which contains a mixture of $CD4^+$ and $CD8^+$ T cells (27). The relationship between TLSs and tumor associated histopathological parameters has been investigated, and the results are contradictory. The presence of TLSs in primary tumors from 225 melanoma patients correlates with good clinical characteristics (28). TLS presence, on the other hand, correlates with higher tumor grade, stage but has no effect on survival in other cancers (29). Such inconsistencies may be due to TLS's mature state. In mature TLSs, B cells can display anti-tumor immune functions by presenting tumor-derived antigens to CD8+ T cells (30). In immature TLSs (lymphocyte aggregates, primary lymphoid follicles), B cells may produce molecules that can be released in the tumor microenvironment or expressed on their membrane, thereby weakening the anti-tumor immune response (30).

To further analyze the mechanism of faster growth of melanoma in *IKZF1* overexpression transgenic mice, we stained the tumor tissues of the 2 groups with HE and counted the number of TLSs in the tumor tissues. Compared with WT mice, the number of immature TLSs in the transplanted tumors of *IKZF1* transgenic mice increased significantly. These immature TLSs do not exert the function of anti-tumor immunity. Immature TLS formation was increased in tumor tissues of *IKZF1* transgenic mice after tumor bearing, possibly due to an

increase in immature lymphocytes released by bone marrow stimulated by chronic inflammation caused by tumor cells and an increase in immune-suppressing regulatory cells.

TLSs in tumor tissues consist of T cells, B cells, dendritic cells (DCs), FDCs, follicular helper T cells (TFH), stromal fibroblasts, and high endothelial venules (HEVs) (27,31,32). IKZF1 is a transcription factor required for lymphocyte development and controls the specificity and differentiation of lymphocytes (33,34). Many regulatory activities during B cell lineage differentiation are also controlled by *IKZF1* and other major B cell transcription factors (35). *IKZF1* also affected the differentiation of myeloid cells. *IKZF1* deficient mice showed abnormal bone marrow development, including a loss of DCs and an increase in basophils and megakaryocytes (36-38). We speculate that *IKZF1* may increase the formation of immature TLSs in transplanted tumors by affecting the differentiation of T cells, and B cells, and increasing the immune suppressive cells. However, the specific mechanism of *IKZF1* in TLS regulation still needs to be further clarified.

Conclusions

IKZF1 did not affect the proliferation of melanoma cells. Using an *IKZF1* transgenic mouse model, it was found that *IKZF1* is a key driver gene in the formation of immature TLS in the melanoma microenvironment. Turning *IKZF1*-driven immature TLS into mature TLS is the next major research task.

Acknowledgments

Funding: This study was supported by the National Natural Science Foundation of China (No. 82002922).

Footnote

Reporting Checklist: The authors have completed the ARRIVE reporting checklist. Available at https://tcr.amegroups.com/article/view/10.21037/tcr-22-1759/rc

Data Sharing Statement: Available at https://tcr.amegroups.com/article/view/10.21037/tcr-22-1759/dss

Conflicts of Interest: All authors have completed the ICMJE uniform disclosure form (available at https://tcr.amegroups.com/article/view/10.21037/tcr-22-1759/coif). The authors have no conflicts of interest to declare.

Ethical Statement: The authors are accountable for all aspects of the work in ensuring that questions related to the accuracy or integrity of any part of the work are appropriately investigated and resolved. Animal experiments were performed under a project license (No. SH9H-2020-A276-1) granted by the Experimental Animals Ethics Committee of Shanghai 9th People's Hospital, Shanghai Jiao Tong University School of Medicine, in compliance with the national guidelines for the care and use of animals.

References

1. Willsmore ZN, Coumbe BGT, Crescioli S, et al. Combined anti-PD-1 and anti-CTLA-4 checkpoint blockade: Treatment of melanoma and immune mechanisms of action. Eur J Immunol 2021;51:544-56.
2. Robert C, Schachter J, Long GV, et al. Pembrolizumab versus Ipilimumab in Advanced Melanoma. N Engl J Med 2015;372:2521-32.
3. Topalian SL, Hodi FS, Brahmer JR, et al. Safety, activity, and immune correlates of anti-PD-1 antibody in cancer. N Engl J Med 2012;366:2443-54.
4. Hodi FS, O'Day SJ, McDermott DF, et al. Improved survival with ipilimumab in patients with metastatic melanoma. N Engl J Med 2010;363:711-23.
5. Liu X, Hogg GD, DeNardo DG. Rethinking immune checkpoint blockade: 'Beyond the T cell'. J Immunother Cancer 2021;9:e001460.
6. Ribas A, Wolchok JD. Cancer immunotherapy using checkpoint blockade. Science 2018;359:1350-5.
7. Helmink BA, Reddy SM, Gao J, et al. B cells and tertiary lymphoid structures promote immunotherapy response. Nature 2020;577:549-55.
8. Cabrita R, Lauss M, Sanna A, et al. Tertiary lymphoid structures improve immunotherapy and survival in melanoma. Nature 2020;577:561-5.
9. Petitprez F, de Reyniès A, Keung EZ, et al. B cells are associated with survival and immunotherapy response in

sarcoma. Nature 2020;577:556-60.
10. Posch F, Silina K, Leibl S, et al. Maturation of tertiary lymphoid structures and recurrence of stage II and III colorectal cancer. Oncoimmunology 2017;7:e1378844.
11. Schumacher TN, Thommen DS. Tertiary lymphoid structures in cancer. Science 2022;375:eabf9419.
12. Siliņa K, Soltermann A, Attar FM, et al. Germinal Centers Determine the Prognostic Relevance of Tertiary Lymphoid Structures and Are Impaired by Corticosteroids in Lung Squamous Cell Carcinoma. Cancer Res 2018;78:1308-20.
13. Calderaro J, Petitprez F, Becht E, et al. Intra-tumoral tertiary lymphoid structures are associated with a low risk of early recurrence of hepatocellular carcinoma. J Hepatol 2019;70:58-65.
14. Mitchell JL, Seng A, Yankee TM. Ikaros, Helios, and Aiolos protein levels increase in human thymocytes after β selection. Immunol Res 2016;64:565-75.
15. Yang L, Luo Y, Wei J. Integrative genomic analyses on Ikaros and its expression related to solid cancer prognosis. Oncol Rep 2010;24:571-7.
16. Yoshida T, Georgopoulos K. Ikaros fingers on lymphocyte differentiation. Int J Hematol 2014;100:220-9.
17. Ochiai K, Yamaoka M, Swaminathan A, et al. Chromatin Protein PC4 Orchestrates B Cell Differentiation by Collaborating with IKAROS and IRF4. Cell Rep 2020;33:108517.
18. Dumortier A, Kirstetter P, Kastner P, et al. Ikaros regulates neutrophil differentiation. Blood 2003;101:2219-26.
19. He LC, Gao FH, Xu HZ, et al. Ikaros inhibits proliferation and, through upregulation of Slug, increases metastatic ability of ovarian serous adenocarcinoma cells. Oncol Rep 2012;28:1399-405.
20. Zhang Z, Xu Z, Wang X, et al. Ectopic Ikaros expression positively correlates with lung cancer progression. Anat Rec (Hoboken) 2013;296:907-13.
21. Lu G, Middleton RE, Sun H, et al. The myeloma drug lenalidomide promotes the cereblon-dependent destruction of Ikaros proteins. Science 2014;343:305-9.
22. Barcellos-Hoff MH. Remodeling the irradiated tumor microenvironment: The fifth R of radiobiology? Increasing the therapeutic ratio of radiotherapy. Springer, 2017:135-49.
23. Michalinos A, Tsaroucha AK, Lambropoulou M, et al. Glycoprotein non-metastatic melanoma B expression after hepatic ischemia reperfusion and the effect of silibinin. Transl Gastroenterol Hepatol 2020;5:7.
24. Chen DS, Mellman I. Elements of cancer immunity and the cancer-immune set point. Nature 2017;541:321-30.
25. Uson Junior PLS, Liu AJ, Sonbol MB, et al. Immunotherapy and chimeric antigen receptor T-cell therapy in hepatocellular carcinoma. Chin Clin Oncol 2021;10:11.
26. Tugues S, Ducimetiere L, Friebel E, et al. Innate lymphoid cells as regulators of the tumor microenvironment. Semin Immunol 2019;41:101270.
27. Sautès-Fridman C, Petitprez F, Calderaro J, et al. Tertiary lymphoid structures in the era of cancer immunotherapy. Nat Rev Cancer 2019;19:307-25.
28. Martinet L, Le Guellec S, Filleron T, et al. High endothelial venules (HEVs) in human melanoma lesions: Major gateways for tumor-infiltrating lymphocytes. Oncoimmunology 2012;1:829-39.
29. Hill DG, Yu L, Gao H, et al. Hyperactive gp130/STAT3-driven gastric tumourigenesis promotes submucosal tertiary lymphoid structure development. Int J Cancer 2018;143:167-78.
30. Kroeger DR, Milne K, Nelson BH. Tumor-Infiltrating Plasma Cells Are Associated with Tertiary Lymphoid Structures, Cytolytic T-Cell Responses, and Superior Prognosis in Ovarian Cancer. Clin Cancer Res 2016;22:3005-15.
31. Yamakoshi Y, Tanaka H, Sakimura C, et al. Immunological potential of tertiary lymphoid structures surrounding the primary tumor in gastric cancer. Int J Oncol 2020;57:171-82.
32. Di Caro G, Bergomas F, Grizzi F, et al. Occurrence of tertiary lymphoid tissue is associated with T-cell infiltration and predicts better prognosis in early-stage colorectal cancers. Clin Cancer Res 2014;20:2147-58.
33. Georgopoulos K, Moore DD, Derfler B. Ikaros, an early lymphoid-specific transcription factor and a putative mediator for T cell commitment. Science 1992;258:808-12.
34. Georgopoulos K, Bigby M, Wang JH, et al. The Ikaros gene is required for the development of all lymphoid lineages. Cell 1994;79:143-56.
35. Hu Y, Zhang Z, Kashiwagi M, et al. Superenhancer reprogramming drives a B-cell-epithelial transition and high-risk leukemia. Genes Dev 2016;30:1971-90.
36. Malinge S, Thiollier C, Chlon TM, et al. Ikaros inhibits megakaryopoiesis through functional interaction with GATA-1 and NOTCH signaling. Blood 2013;121:2440-51.
37. Rao KN, Smuda C, Gregory GD, et al. Ikaros limits basophil development by suppressing C/EBP-α expression.

Blood 2013;122:2572-81.
38. Wang JH, Nichogiannopoulou A, Wu L, et al. Selective defects in the development of the fetal and adult lymphoid system in mice with an Ikaros null mutation. Immunity 1996;5:537-49.

(English Language Editor: C. Betlazar-Maseh)

Cite this article as: Yin S, Zhang C, Gao F. Immature tertiary lymphoid structure formation was increased in the melanoma tumor microenvironment of *IKZF1* transgenic mice. Transl Cancer Res 2022;11(7):2388-2397. doi: 10.21037/tcr-22-1759

